23rd International Congress on Sound & Vibration
Athens, Greece 10-14 July 2016
ICSV23

ACTIVE VIBRATION CONTROL BY PIEZOCERAMIC ACTUATORS OF A CAR FLOOR PANEL

Dario Magliacano and Massimo Viscardi

University of Naples, Naples, Italy
email: darius6591@hotmail.it

Ignazio Dimino and Antonio Concilio

Adaptive Structures Division, C.I.R.A. – The Italian Aerospace Research Centre, Capua (CE), Italy
email: i.dimino@cira.it

Active vibration control was successfully tested in many automotive and aeronautical applications. The main purpose of this work is the implementation and experimental investigation of the applicability and efficiency of an active vibration control (AVC) concept for vibration reduction in an automobile passenger compartment. In the contest of the presented activity, the floor panel of a medium-class test car has been studied as test case for an AVC implementation based on the use of piezoelectric actuators. A preliminary numerical activity has been performed for the correct evaluation of the dynamic behaviour of the system under the specific external disturbance spectra; based upon this information, a procedure for the correct positioning of sensors and actuators devices has been implemented. The following experimental activity has then been dedicated to the implementation of both SISO (Single Input Single Output) and SIMO (Single Input Multiple Output) feedforward control applications, under simulated conditions of external disturbance field. The principal results that will be discussed within the paper show a good ability of the actuation system to manage the control signals in terms of vibrational energy; this circumstance, candidate piezoelectric patches as adequate actuation devices. Under the specific control point of view, it appears evident that SISO results are appreciable only at error sensor, while uncontrollable conditions emerge at other locations. This limitation may be partially overcome with the SIMO architecture, but a review of the main limitations concerning this architecture are also presented.

1. Introduction

1.1 Active control applications

There is always a stronger and more insistent research, by producers, of new technical solutions and control methods for noise and vibration level reductions, with better performances and more flexible operational capabilities. Areas of application that now show an irreversible trend towards the adoption of active sound and/or vibration control systems are:

- Transport vehicles (aircrafts, cars, trains, ships), concerning the improvement of interior comfort and outdoor pollution;
- Civil engineering structures (skyscrapers, towers, workshops, bridges, industrial complexes) regarding earthquake protection, the reduction of the effects due to noise and vibrations induced by road and rail traffic, by the wind, and by the presence inside and/or outside of large rotary machines, such as turbines, pumps or compressors;
- Household appliances (refrigerators, washing machines and dishwashers).

1.2 Sources of interior noise and vibrations in automotive

With reference to the first class of systems and specifically, to automotive vehicle, it can be stated that a variety of independent noise sources impact on passengers' perceived noise in vehicles. These sources may be transmitted via a variety of structural paths, and then radiated acoustically into the cabin (structural-borne noise) or acoustically generated and propagated by airborne paths (air-borne noise). The major contributors may be thus distinguished in:

- Tire rolling noise: the interaction between tires and ground generates broadband vibrations that are transmitted to the structure. This phenomenon is more remarkable at low temperatures, due to the stiffening of the tire. Working on suspensions could severely affect performances, while the use of a structural shock absorber could heavily increase the weight; so, here is the need to develop an active control system.
- Engine noise: mechanic and chemical processes inside the engine generate vibrations and therefore noise, which is transmitted to the cockpit. In addition, new low-power engines need a design that causes greatest noise at equal thrust.
- Aerodynamic noise: the "noise vortices" are caused by the interaction between a fluid (air) and a non-aerodynamic body (car). The frequency of detachment of these Von Karman vortices generates unstable forces that produce both broadband and tonal noise. This noise is transmitted to the structure, that vibrates and transfers it into the interior.

Very often, the attenuation of these noise sources require a substantial increment of the mass and stiffness of structural elements present along the noise transmission path, with a consequent deterioration of other vehicle parameters (consumption, performances, drivability, ...); also because, these technologies are not able to adapt their performance to the specific condition and are so designed for the worst condition to be faced with. The engineering challenge of the lightweight structure need, by this point of view, new solution that may be partially represented by those recognized as "active technologies".

2. Active control with feedforward strategy

2.1 Introduction

The reduction of interior noise through active devices has been a research topic for more than 50 years. Rubber and hydro mounts are the standard tool to isolate the engine and the transmission from the chassis. Rubber isolators work well (in terms of isolation) when the rubber exhibits low stiffness and little internal damping. Little damping, however, leads to a large resonance peak which can manifest itself in excessive engine movements when this resonance is excited (front end shake). These movements must be avoided in the tight engine compartments of today's cars. A low stiffness, while also giving good isolation, leads to a large static engine displacement and to a low resonance frequency (which would adversely affect the vehicle comfort and might coincide with resonance frequencies of the suspension system). Classical mount (or suspension) design therefore tries to achieve a compromise between the conflicting requirements of acceptable damping and good isolation. It is clear that this, as well as other passive vibration control measures, is a trade-off design method in which the properties of the structure must be weighted between performance and comfort. An attractive alternative that overcomes the limitations of the purely passive approach is the use of active noise and vibration control techniques (ANC/AVC). The basic idea of ANC and AVC is to superimpose the unwanted noise or vibration signals with a cancelling signal of exactly the same magnitude and a phase difference of 180° (i.e. the ''anti-noise" principle of Lueg (Lueg, 1933)) [1].
A feedforward control strategy is possible only if there is a preliminary information about the excitation of the primary source to be controlled; if that is not possible, feedback control strategies are preferred instead. Typically, the primary excitation cannot be directly measured and a reference sensor is used to detect the primary wave. The signal, from the reference sensor, is in turn transmitted to

an electronic controller, which then controls the secondary excitation (control actuator); the main purpose is then to design a controller capable to minimize the output of one or many error sensors. More recently, the active controllers are implemented in digital signal processor (DSP) boards. This gives rise to the need for accounting inevitable delays associated with the controller, due to both the DSP processing time and the presence of amplifiers in the feedforward control scheme. The feedforward control of random noise, therefore, is effective only if the delay in the path from the reference sensor to the error (via the controller) is less than the time that the elastic wave takes to travel the same distance through the structure; this is generally referred to as "causality constraint". Conversely, this effect is largely manageable when the incident wave is of deterministic nature (e.g., harmonics). The current paper considers the reduction of car rear under-seat panel-induced vibrations. A pure feedforward strategy (with no adaptation), using piezoelectric patches as control actuators is implemented and experimented on the test article. The criterion of least squares (optimal control) is applied to estimate the performance of feedforward control systems using different local control schemes with one or more secondary sources and one or more error sensors.

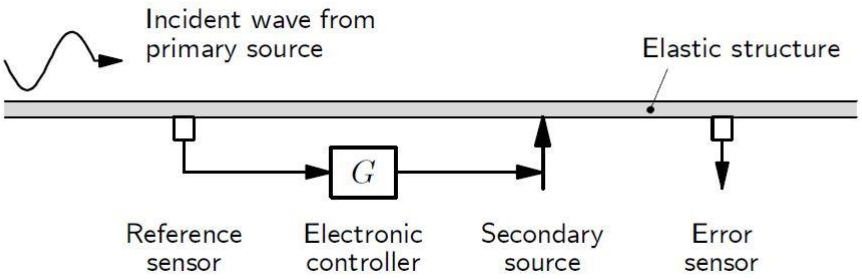

Figure 1: Feedforward control system to control the propagation of a wave within an elastic structure. [2]

2.2 Optimal control

Assuming a linear behaviour of all the parts of the system (structural, electrical and piezoelectric) and all the signals are in the respective stationary states, the frequency-domain complex output of the error sensor (y) is the complex output overlapping due to only the primary excitation (y_d) and to exclusively the secondary one (y_c). The error signal can then be expressed in terms of complex concentrated force amplitude (v_d) and complex amplitude of the voltage applied to the piezoelectric (v_c):

$$y = y_d + y_c = H_d v_d + H_c v_c$$

In the previous equation, H_d represents the so-called primary path, i.e. the FRF from the primary source to the error sensor, while H_c is the secondary path, i.e. the FRF between the secondary source and the error sensor. It therefore assumes that the signals relating to primary and secondary sources are perfectly consistent, that is there are no other unrelated signals (such as noise); therefore, the acceleration signal can be cancelled at any frequency by introducing a secondary inputs equal to:

$$v_c^{min} = -\frac{H_d}{H_c} v_d$$

Obviously, the FRF of the secondary path should not be null to prevent an optimal control with divergent secondary input; this singular condition is avoided by introducing damping into the system. Generally, the control system consists of multiple secondary sources and multiple error sensors (MIMO system); in this case, the equation can be rewritten as:

$$\{y\} = [H_d]\{v_d\} + [H_c]\{v_c\}$$

Note that the (i, j)-th element of the $[H_c]$ matrix is the FRF between the i-th error sensor and the j-th secondary source. If the number of error sensors and the number of secondary sources are equal, the optimal vector of the secondary inputs (i.e., the vector that eliminates the output of all error sensors) is given by:

$$\{v_c^{min}\} = -[H_c^{-1}][H_d]\{v_d\}$$

In many cases, however, the number of error sensors and that of secondary sources are not equal; in such cases, the optimal secondary input can be calculated by minimizing the error through the application of the least squares criterion, in the form:

$$J = \{y^H\}[W_y]\{y\} + \{v_c^H\}[W_c]\{v_c\}$$

Where $[W_y]$ is the weight matrix of the errors and $[W_c]$ is the gain weight matrix; through the first, some of the error signals may have priority over others. The error criterion can be written in the so-called "Hermitian quadratic form":

$$J = \{v_c^H\}[A]\{v_c\} + \{v_c^H\}\{b\} + \{b^H\}\{v_c\} + c$$

Where single terms are given by:

$$[A] = [H_c^H][W_y][H_c] + [W_c]$$
$$\{b\} = [H_c^H][W_y][H_d]\{v_d\}$$
$$c = \{v_d^H\}[H_d^H][W_y][H_d]\{v_d\}$$

The cost function J has a unique minimum if [A] is not singular and this is guaranteed if [A] is positive defined; to verify this condition, the weight matrices $[W_y]$ and $[W_c]$ must be positive defined. Downstream of this, the control inputs that minimize the error criterion are:

$$\{v_c^{min}\} = -[A^{-1}]\{b\}$$

While the minimum of the error criterion is:

$$J^{min} = c - \{b^H\}[A^{-1}]\{b\}$$

3. System dynamic characterization and actuator's location

The test article of the present activity, as previously stated, is represented by the rear floor panel of a car; the squared box in figure 2 give evidence of the specific area.

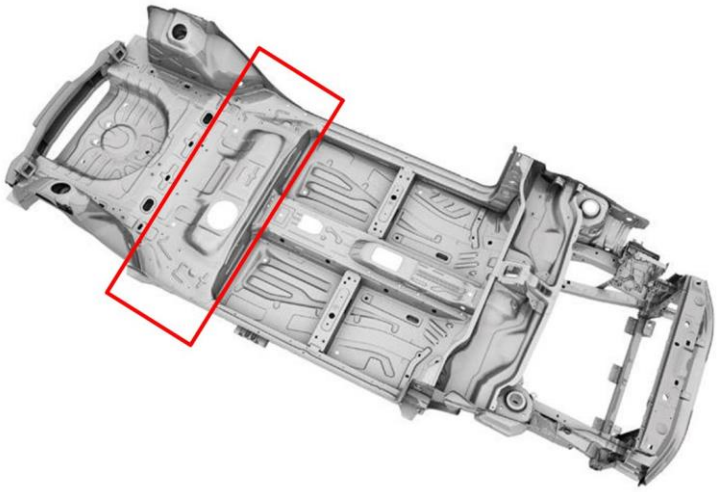

Figure 2: Car floor panel.

As a first activity, a numerical modal analysis of this component has been carried out from 0 Hz to 300 Hz using the software MSC Nastran; it revealed the presence of six normal modes of vibration within that range, whose relative frequencies are reported in next Table 1. It is important to underline that the numerical model include the mass and stiffness effect of the rest of the car body floor that has been condensed during a preliminary model refinement.

Table 1: Numerical proper modes of vibration.

Mode	1	2	3	4	5	6
Frequency [Hz]	152.79	204.56	236.21	259.39	259.49	283.11

Relative strain distribution contour plots are presented in the next pictures (figures 3-8).

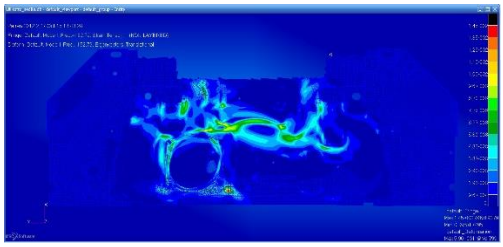

Figure 3: Strains – mode 1.

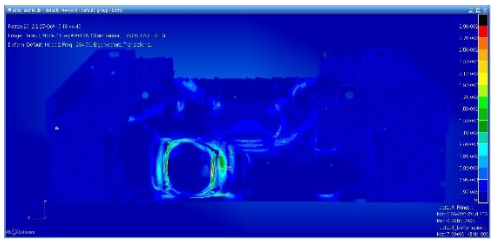

Figure 4: Strains – mode 2.

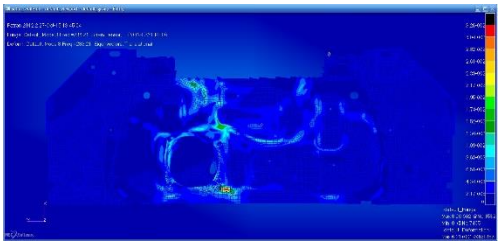

Figure 5: Strains – mode 3.

Figure 6: Strains – mode 4.

Figure 7: Strains – mode 5.

Figure 8: Strains – mode 6.

4. Experimental setup

The experimental activities have been carried out on the rear car floor panel of the real car at the C.I.R.A. facilities.

The primary excitation device is represented by a shaker (Figure 10), suspended with a hook and interfaced to the trunk of the car. Realistically, the primary excitation should originate from an area close to the suspensions; however, because of the difficulty of access to this zone, downstream of the detection of a good transmissibility between the area of the trunk and that of the rear floor panel, it was opted for this solution.

Pure sine signals where used as excitation spectra during the first part of the activity; the main results herein presented refers to the 300 Hz pure tone (this frequency does not coincide with any normal mode and has been focused as significant frequency related to real operative conditions).

The error and monitoring sensor set-up consisted of 44 accelerometers installed on the rear floor panel (figure 9), even if has been noted that this acquisition and control grid has not been used, in its entirety, for the purpose of the tests discussed here, but it has been prepared as necessary for additional tests not covered in this paper. 5 locations were then selected for the piezoelectric patches (control sources), on the basis of specific strain contours at the selected control frequencies.

Control system consisted of a dSpace multichannel control board where two feedforward control algorithms have been implemented.

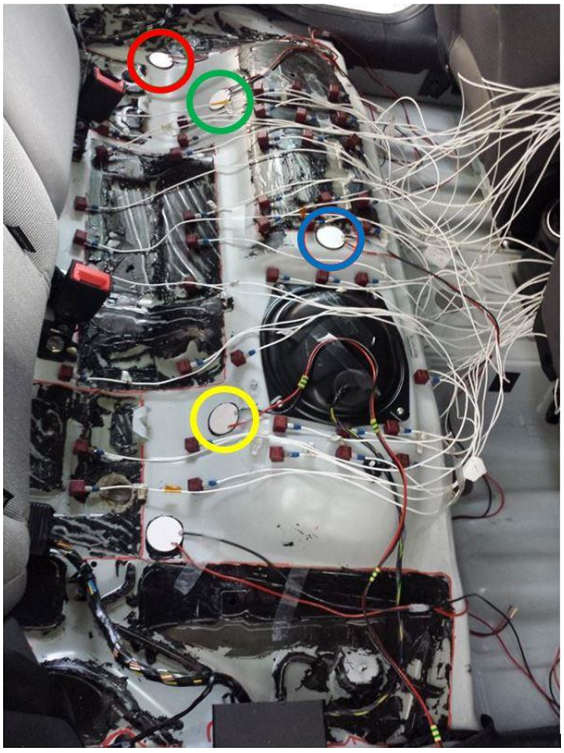

Figure 9: Experimental setup.

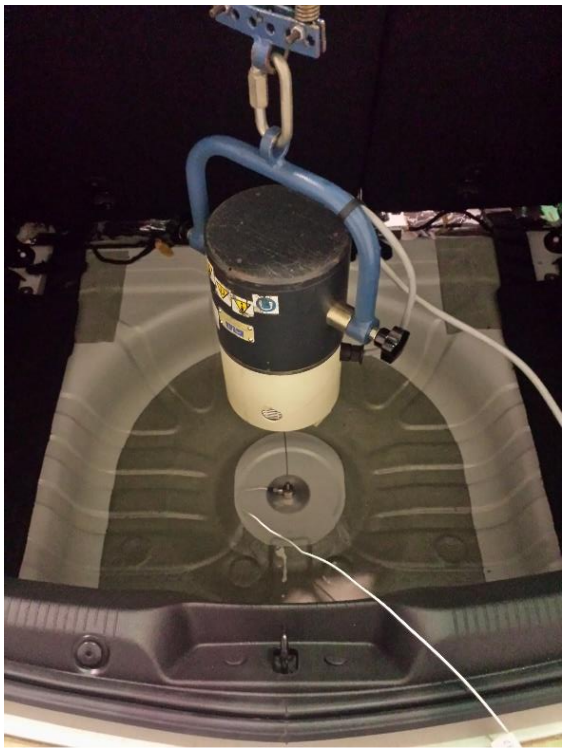

Figure 10: Excitation device.

5. Experimental results

As already described in the introduction chapter, the present study was mainly targeted at the verification of the piezoelectric patches ability to introduce inside the system the adequate amount of energy to control the primary disturbance field preliminary evaluated on the basis of road test.
To stress this verification a pair of locations were chosen very far each other; in the specific, it was decided to use the piezoelectric "3" (circled in blue in Figure 9) as sensor and the piezoelectric "5" (circled in red in Figure 9) as control device.
To verify the ability of control signal to counteract the primary one the phase of the corresponding actuating signal has been calculated with the formula:

$$\text{control phase (in degrees)} = 180 - (B2 - B1)$$

where:

- B1 is the phase of the excitation device – sensor FRF;
- B2 is the phase of the control device – sensor FRF.

Under this condition, it has been verified that a control voltage as small as 35 V was able to generate a secondary control field causing a strong reduction of overall vibration at the error sensor location. This circumstance represented an important preliminary results, because such a voltage level does not imply the use of big and expensive power supply but can be easily managed with light and cheap logic technology.

5.1 SISO application

For the first experimental application discussed further below, after the preliminary tests, a SISO architecture was implemented. During these test, different pair of sensors and actuators were tested. All the tests were performed under the application of a sinusoidal excitation signal, and as a general consideration it can be stated that, in the best condition, the controlled response was detected equal to 21 % of the not controlled one (Figure 12); in other words, the obtained reduction of the response equal has been always greater that 13.6 dB.

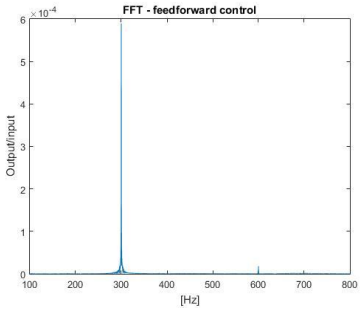

Figure 11: Signal Fourier Transform.

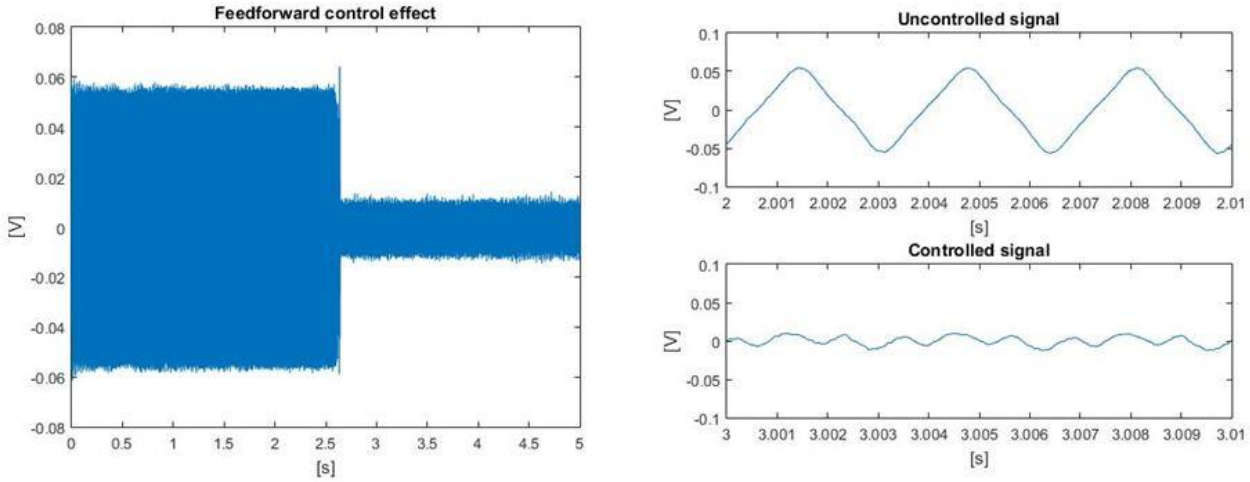

Figure 12: Effect of the feedforward control (left) and zoom (right).

This result appears satisfactory, but also expected, because under a theoretical point of view, the control system is always able to manage the right phase of the control signal to perfectly be in opposition of phase at the error sensor. Unfortunately, this circumstance may generate a possible increment of the vibration level at other location not managed within the control algorithm; see, in example what has been measured under this configuration where piezoelectric "3" (circled in blue in Figure 9) as error sensor, the piezoelectric "4" (circled in green in Figure 9) as monitoring sensor and the piezoelectric "2" (circled in yellow in Figure 9) as control device.

Under the above conditions, it has been checked an amplification of +22.8 dB of the vibrational level in correspondence of the monitoring sensor; but also this circumstance was expected because both the optimum phase or amplitude parameters referred to the error sensor may have a complete opposite effect at other locations (in this case, in example, the increment is more significant at monitoring station than the reduction at the error location, due to the proximity to the actuation source).

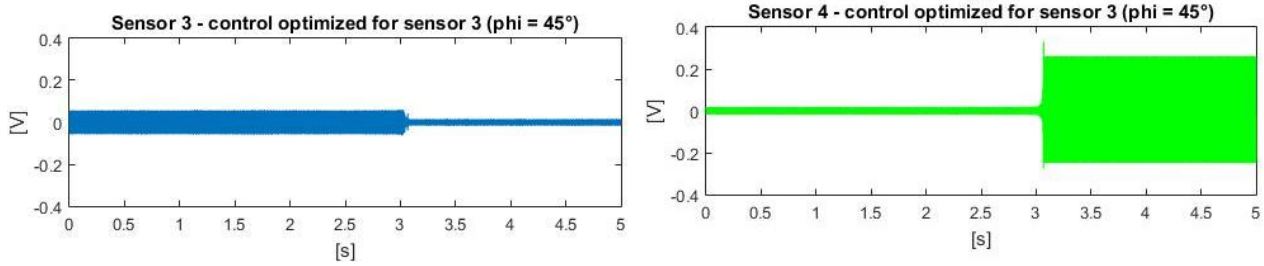

Figure 13: Effect of the SISO feedforward control at error and monitoring sensors.

5.2 SIMO application

The second application, in addition to the above, provides the presence of two error sensors (both sensor 3 and 4 have been introduced in the control low); in this circumstance, a reduced level of the controlled response may be measured at both locations, but relative value (approx. -2.5 dB in both sensors) is much reduced if compared at SISO configuration.

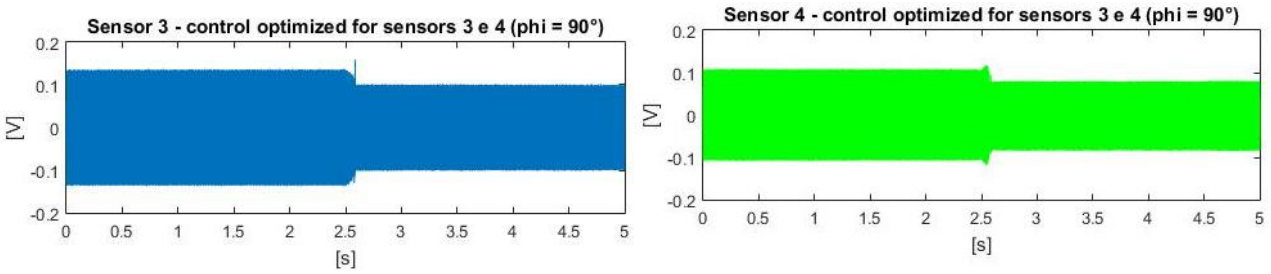

Figure 14: Effect of the feedforward control at error sensors 3 and 4.

Also this behaviour was expected because the searched minimum vibration level at both sensors requires a compromise of the optimal amplitude and phase of the control signal.

6. Conclusions and future planned activities

The present study gathered essential data and parameters for the design of noise and vibration active control architectures in the automotive sector. Preliminarily numerical and experimental activities have shown the opportunity to use piezoelectric devices both as sensor and actuators because they have shown a good sensibility when used as sensors and an adequate transmitted energy when used as actuators. SISO and SIMO test herein presented have to be considered as preliminary approach to validate the physical architecture; it is evident that a MIMO feedforward approach or a feedback strategy will be realistic implemented on the basis of availability of a correlated reference signal or not.

REFERENCES

1 Svaricek, F., Fueger, T., Karkosch, H., Marienfeld, P. and Bohn, C. *Automotive Applications of Active Vibration Control*, (2010).

2 Nijhuis, M. O. *Analysis tools for the design of active structural acoustic control systems*, (2003).

3 Magliacano, D. *Controllo attivo di rumore e vibrazioni in ambito automotive*, (2016).

4 Marino, N., Isernia, G., Viscardi, M. and Isernia, M. *Progettazione e sviluppo di un sistema di controllo attivo del rumore interno ad un velivolo dell'aviazione generale*, (2001).

5 Lecce, L., Viscardi, M. and Zumpano, G. Multifunctional system for active noise control and damage detection on a typical aeronautical structure, *Proceedings of SPIE - The International Society for Optical Engineering*, **4327**, 201-212, (2001).

6 Dimino, I. and Aliabadi, F. *Active control of aircraft cabin noise*, (2015).

7 Preumont, A. *Mechatronics: Dynamics of Electromechanical and Piezoelectric System*, (2006).

8 Preumont, A. and Seto, K. *Active Control of Structures*, (2008).

9 Leleu, S., Abou-Kandil, H. and Bonnassieux, Y. Piezoelectric actuators and sensors location for active control of flexible structures, *IEEE Transactions on Instrumentation and Measurement*, **50** (6), (2002).